Characterization of large-area silicon ionization detectors for the ACE mission

Brian L. Dougherty[1], Eric R. Christian[3], Alan C. Cummings[2],
Richard A, Leske[2], Richard A. Mewaldt[2], Barrett D. Milliken[1],
Tycho T. von Rosenvinge[3], and Mark E. Wiedenbeck[1]

[1]Jet Propulsion Laboratory, Pasadena,CA911 09
[2]California Institute of Technology, Pasadena, CA 91125
[3]Laboratory for High Energy Astrophysics, NASA/GSFC, Greenbelt, MD 20771

ABSTRACT

Wc report on extensive tests of large-area (1 O cm diameter) high-purity ion-implanted silicon detectors for the Solar Isotope Spectrometer (S1S), and lithium-drifted silicon detectors for the Cosmic Ray Isotope Spectrometer (CRIS), which arc under development for launch on the Advanced Composition Explorer (ACE) mission. Depletion and breakdown characteristics versus bias were studied, as were long-term current and noise stability in a thermally cycled vacuum. Dead-layer and total thickness maps were obtained using laser interferometry, beams of energetic argon nuclei and radioactive sources of alpha particles. Results, selection criteria, and yields arc. presented.

Keywords: large-ama lithium-drifted and high-purity ion-implanted silicon ionization detectors, dead-layers

1. INTRODUCTION

The Advanced Composition Explorer is a NASA mission currently being developed to study the elemental, isotopic and ionic charge-state abundances of particles accelerated on the Sun, within the heliosphere, and in our Galaxy. [1] Among the instruments aboard the ACE spacecraft, the Solar Isotope Spectrometer (S1S) and the Cosmic Ray Isotope Spectrometer (CRIS) will usc coaxial stacks of silicon solid state detectors to make precise measurements of dE/dx versus total energy for energetic nuclei. These measurements, together with trajectory information provided by specialized hodoscopes in front of each stack,[2] will allow the elemental and isotopic abundances of such nuclei to be determined. S1S will be sensitive to solar, anomalous, and interplanetary particles with energies from -10 to -200 McV/nucleon, while CRIS will measure particles of interstellar and galactic origin with energies from -50 to -600 McV/nucleon.

The detectors for both instruments arc fabricated from 10 cm diameter silicon wafers, with thicknesses appropriate for the intended energy ranges. S1S has two stacks of 15 high-purity (HPSi) detectors with 65 cm^2 active areas and with thicknesses ranging from 100 to 1000 μm. CRIS has four stacks of 15 Iithium-drifted (Si(Li)) detectors, all 3 mm thick and with either 57 or 68 cm^2 active areas inside their guard-ring perimeters. The thicknesses of individual detectors, and/or groups of detectors, progresses with depth in each stack, (See Figures 1 and 2.)

In this paper, the manufacture and testing of S1S and CRIS detectors arc reviewed. Fabrication techniques arc briefly described, as are aspects of available silicon crystal quality that limited their yield. Summaries arc provided of depletion and breakdown characteristics, and of the studies undertaken to screen for stability and robustness to ensure operation throughout the course of the ACE mission, which could extend 5 years. Pcrformancc in these basic tests was the main criterion for selecting individual devices for flight, HPSi detectors were limited primarily by narrow usable ranges of voltage between depletion and breakdown. Si(Li) devices were limited mainly by instabilities of noise and leakage current in vacuum.

In addition to the above viability tests, investigations were undertaken to measure the total and active thicknesses of each detector to high precision. This was needed in order to achieve good isotopic resolutions for heavy nuclei incident on a stack, The total thicknesses of the HPSi detectors were mapped with a custom-developed dual laser intcrfcromctcr, while dead-layers were measured using collimated radioactive sources of alpha particles. Beams of penetrating argon nuclei were used to map both the active and total depths of the Si(Li) detectors. Finally, results arc presented which indicate that dead-layer structures arc non-trivial: charge collection efficiencies appear to vary with depth within these “dead” layers.

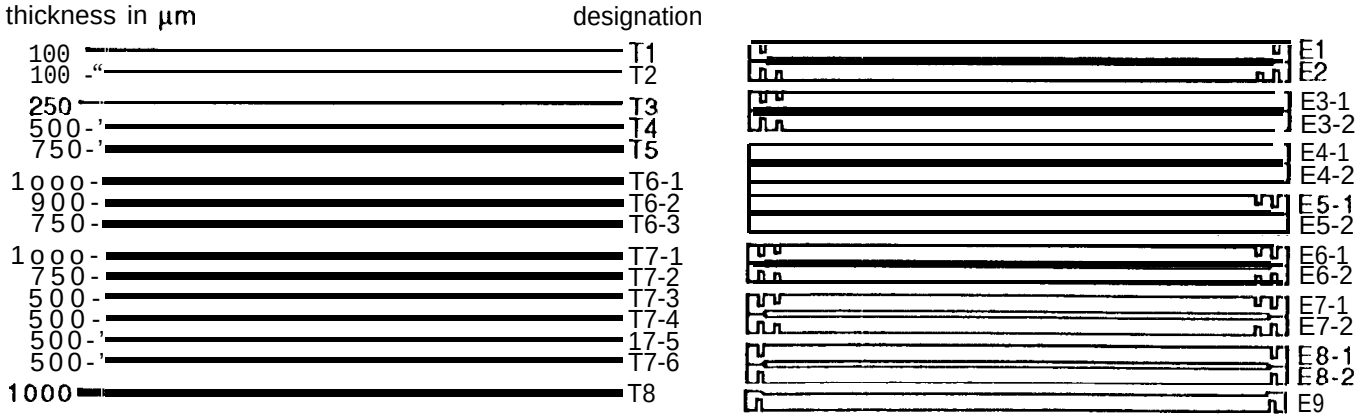

Figure 1. Arrangement of detectors within individual S1S (a) and CRIS (b) stacks. For SIS, detector thicknesses are noted on the left, and designations are on the right. The three detectors that makeup T6 arc connected in parallel, and biased together from onc voltage SUpply. Similarly for T7. Thus, T6 and T7 serve as single devices of thickness 2650 and 3750 μm respectively. The total depth of a S1S stack is about 9.1 mm. For CRIS, the total stack thickness is 45 mm. Single and double-groove detectors appear at different positions, with pairs of detectors mounted back-lo-back. The E3, E4, E5, E6, E7 and E8 pairs arc biased and analyzed together. Signal-processing electronics for both S1S and CRIS utilize custom VLSI components.[3]

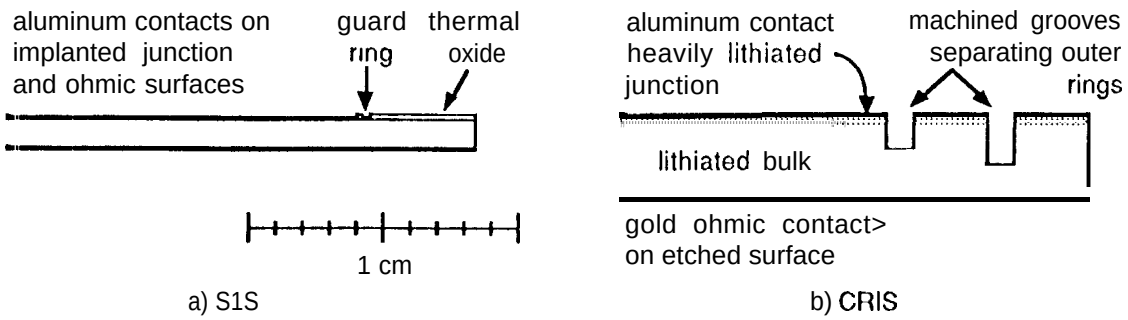

Figure 2. Details of detector structure near the perimeter of a 1000 μm thick S1S HPSi detector (a) and a CRIS Si(Li) detector (b). All detectors arc made from 10 cm diameter crystals. The HPSi surface oxide is not shown to scale. A 50 μm wide guard ring surrounds the HPSi central contact, separated by a 50 μm annulus of oxide. The 1 mm wide Si(Li) grooves arc ultrasonically ground into each wafer, and passivated using photoresist. Si(Li) outer rings arc about 3 mm wide. Electrical connections were made by wire bonding for S1S, and via pressure contacts for CRIS. Scc the text for more details.

2. FABRICATION

As described above, S1S uses only HPSi detectors, while CRIS relics exclusively on Si(Li) devices. In addition to providing detector thicknesses best suited to the energy range of each instrument, this approach separated the dependence on detector suppliers. Furthermore, only a small number of different detector designs arc used in S1S and CRIS. This allowed a degree of modularity and interchangeability which contributed to the successful construction of the instruments and simplified the fabrication procedures for our suppliers.

All detectors underwent a number of quality assurance checks during fabrication. In addition, the detector manufacturers remained in close contact with ACE investigators, receiving feedback on the flight suitability of delivered devices and adjusting the variables of production,

2.1 SIS

The HPSi detectors were made by Micron Semiconductor Ltd. using n-type <111> float-zone silicon, most] y provided by Topsil Semiconductor Materials A/S. Crystal purity varied from wafer to wafer as well as within each wafer; room temperature resistivities varied with location from ~10 to -50 kΩcm, but ~18 kΩcm was typical, These post-processing resistivities arc based on the depletion biases of thicker devices. Requirements were not as stringent for the 100 µm detectors, so silicon of lower purity could bc used, and this material was obtained from Wacker Chemicals Ltd..

Polished and cleaned crystal surfaces were first passivated by thick (roughly 1µm) thermal oxide layers, which were then masked and etched to allow implantation. Each junction was patterned as a nearly circular central region of 65 cm^2 area, surrounded by a single guard ring of 50 µm width separated from the center by an annulus of oxide of similar width. Junctions, as well as ohmic contacts were formed by implantation and annealing: junctions with boron to depths of ~1µm, and ohmic surfaces with arsenic to depths of -0.5 µm. Silica[cd aluminum of thickness 0.2 ± 0.1 µm was then deposited on both surfaces to serve as electrical contacts. All detectors were bonded into custom-designed G 10 mounts, with electrical connections provided by redundant wire bonds to pads on these mounts.

All detectors were evaluated at Caltech as delivery progressed. It was found that a number of the thickest devices were not reaching full depletion before breakdown occurred. This was a consequence largely of non-uniformities in resistivity, as will bc described in more detail below. To ensure the yield of a sufficient number of fully -depleted devices, the manufacturer re-processed some 1000 µm wafers down to 900 µm, and made ncw detectors of 750 pm depth.

2.2 CRIS

The Si(Li) detectors were made at Lawrence Berkeley National Laboratory (LBNL) using p-type <111> ftoat-zone silicon with resistivities of 1 – 3 kΩcm provided by Topsil. To make such material, Topsil doped crystals to the appropriate levels by introducing boron during the actual float-zoning process.

Wafers were first cut, lapped and cleaned. Then lithium was vacuum deposited on onc surface, followed by a drive-in diffusion at 375° C for 15 minutes in an argon atmosphere, Either onc or two grooves of 1 mm width and roughly 1.5 mm depth were then ultrasonically cut to define the boundaries of the central active region and the outer ring(s). On devices with only onc outer ring, the groove inner radius is ≈46.5 mm; for double-groove detectors, a second groove of ≈42.5 mm inner radius was added. (A passivating layer of photoresist was later applied in these grooves.) Acceptor impurities in the crystal bulk were compensated by drifting lithium through the wafer, a process which was performed under carefully controlled temperature, voltage and current conditions. The heavily lithiated surface was then lapped down until its sheet resistance just exceeded 20 Ω, which was earlier determined using alpha particles to correspond to a junction thickness of under -20 µm. Aluminum and gold were vacuum deposited on the junction and ohmic surfaces respectively. The average total detector thicknesses were 2990 ± 30 pm. Further details of the fabrication process may bc found in reference 4.

The two-point resistance of the original aluminized surfaces ranged from a fcw ohms to over 30 Q. Subsequently, additional metallizations of chromium and gold were deposited over the aluminum to reduce this resistance and improve the reliability of the pressure contacts to this surface. Final electrical connections were made by gold-coated dimples on spring-loaded (BeCu) fingers.

3. DEPLETION ANI) BREAKDOWN

3.1 SIS

The HPSi detectors arc biased from their central, junction electrode on] y; i.e. the guard-ring potentials were allowed to "float". The alternative provided fcw advantages, as will be described below. This simplified the choice of devices for the flight instrument, since fewer variables were needed to identify matched sets of detectors.

Preliminary assessments of crystal purity were obtained from capacitance-voltage (and noise-voltage) characteristics. These indicated detectors of generally uniform quality made from high-resistivity silicon. However, more thorough studies employing alpha particles incident on these devices showed that certain regions of many detectors depleted at higher bias, indicative of purity variations within the crystals.

Collimated ^{244}Cm sources of 5 McV alpha-particles were. scanned across the ohmic surface of every detector, and pulse height variations were recorded. Maps were thereby obtained which showed distinctive patterns associated with incomplete depletion. The bias dcpcndcncc of these maps was noted, and full depletion was determined when an approximately uniform, featureless response was obtained, Figure 3 shows a series of pulse-height contour maps for a particular 1000 μm thick detector. In 3a), acquired with a 90 V bias, deep "holes" in response arc seen near the middle of the detector. These holes get progressively shallower with bias, until full depletion occurs near 120 V.

Full depletion biases obtained in this manner varied greatly among similar detectors. Depletion voltages for the 1000 pm devices ranged from 110 to 280 V. There remained a general trend, however, that depletion voltages tended to increase with detector thickness.

Breakdown voltages were clearly revealed by rapid increases of noise and/or current. By actively and independently biasing the guard rings, the voltages at which current run-away occurred could often be delayed by tens of volts. But noise levels still worsened at biases beyond the breakdown voltages found using floating guard rings. Usually, growing noise levels were visible on an oscilloscope display of the electronics baseline before any current increase could be detected.

The 1000pm devices broke down anywhere from 100 to 300 V. Similar factor-of-three variability was found in the thinner detectors. Out of nearly 60 detectors delivered with thicknesses of 750 μm or greater, half broke down before depleting over their full area. The thinner detectors fared much better. Only 1 out of 37 devices with depths of 250 and 500 pm failed in this way. For the 100pm detectors, 5 out of 18 broke down early. Figure 4 shows the viable range of biases for detectors with thicknesses of 500 μm and above.

The selection of detectors suitable for flight was largely constrained by the available bias range limited from below by depletion and from above by breakdown. However, additional factors came into play. (1) The original design for a S1S stack had detectors T], T2, T3 and T4 with thicknesses as shown in Figure 1a, and T5 through T8 all as thick as possible, preferably 1000 pm. (2) Wc wished to create two stacks for S1S which contained the same progression of detector thicknesses. (3) The voltage supplies on the flight instrument arc of limited range: T5 through T8 arc programmable from 100 to 250 V only. This was done to allow finer adjustable control (64 steps) within the range of anticipated operating biases. (4) Since the T6 and T7 groups arc biased with single voltage supplies, groups of detectors that operate within the same bias range had to be used. (5) To help ensure good charge collection efficiency and minimize recombination 1OSSCS or ballistic deficits for all ions stopping throughout the depth of any detector, the minimum voltage had to be at least 20 V over the depletion bias.

3.2 CRIS

Depletion biases for the Si(Li) detectors were checked at LBNL by rapidly scanning alpha sources across their ohmic surfaces, and were found 10 be in the 60 – 120 V range. These devices were tested at biases up to 500 V, and in general the leakage currents and noise levels stayed within usable limits. In flight, all detectors will be operated at 400 V.

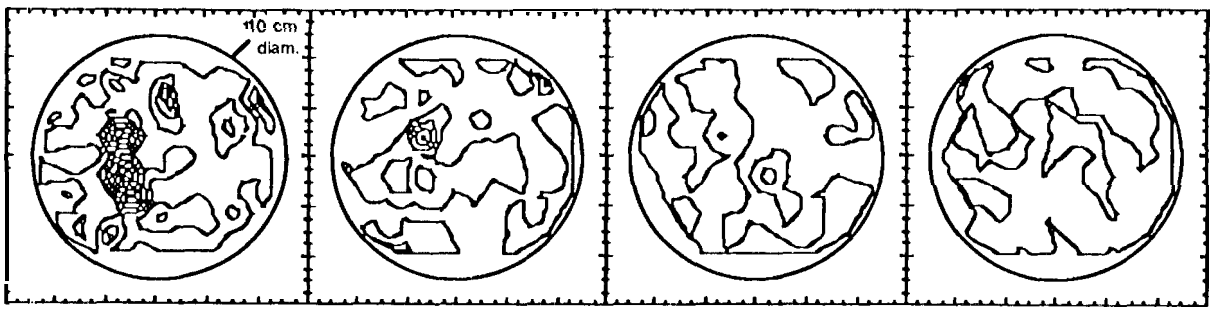

Figure 3. Contour maps of ^{244}Cm alpha particle pulse heights obtained with a 1000 μm thick S1S HPSi detector. (Note, S1S active areas arc 9.2 cm in diameter, and the scale of each frame is 12 x 12 cm.) The alpha source was moved across the ohmic surface of this detector to positions on a 9 mm triangular grid. Contours arc spat.cd by ≈0.6 % of full-height pulses, equivalent to a ≈0.2 μm change in dead layer thickness. The two adjoined, densely-lirrcd hexagons near the center in (a) indicate large deficits in the collected charge (at two grid positions). These "holes", duc to incomplete depletion, rapidly become shallower at 110 V in (b), and nearly disappear at 120 V in (c). Other irregularities in pulse height also improve, and the response map becomes more uniform, At 170 V in (d) the contours fluctuate near the limit of precision for these measurements.

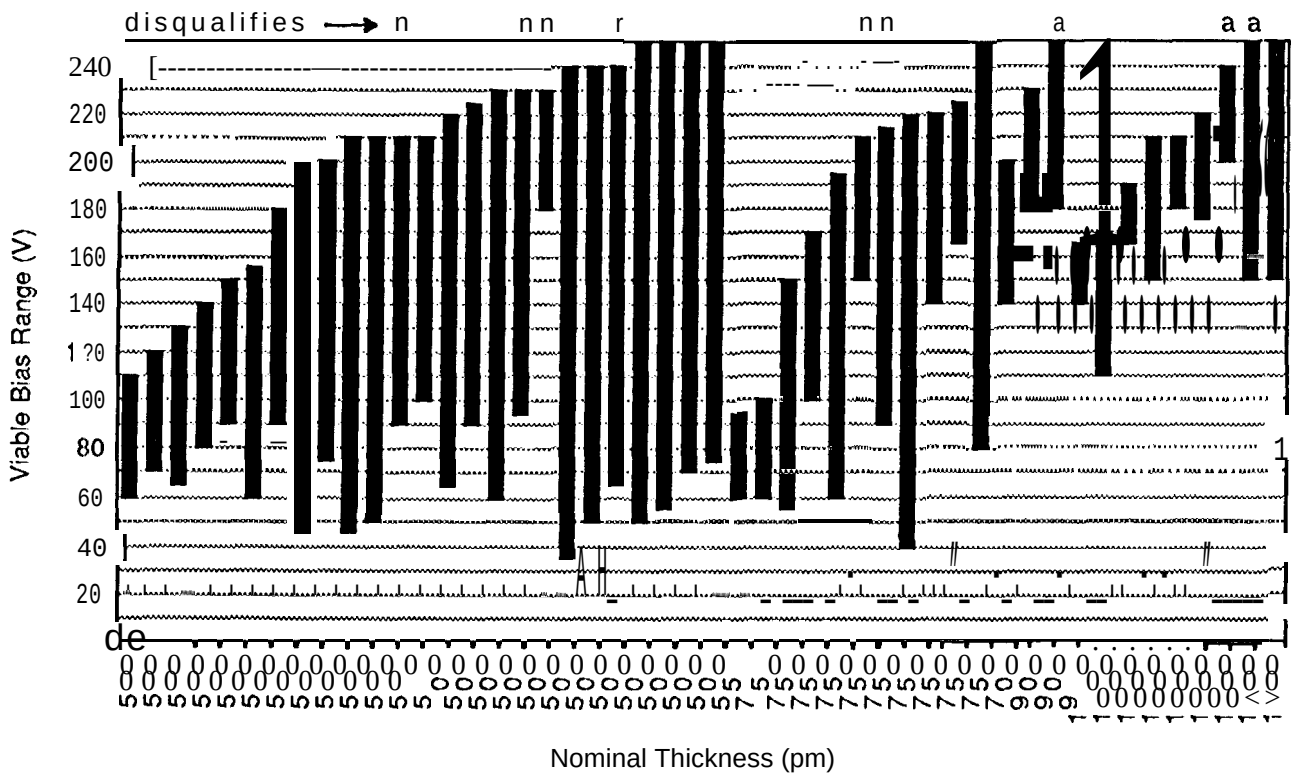

Figure 4. Viable bias ranges (between depletion and ~10 V below breakdown) for SIS HPSi detectors with thicknesses of 500 μm or larger. Detectors which had lcss than 20 V of viable range arc not plotted. The "disqualifier" symbols above particular columns indicate devices with poorer noise performance (n), or with significant dead-layer variability found in alpha particle maps of the surface response (a).

4. CURRENT ANI) NOISE STABILITY IN A THERMALLY CYCLED VACUUM

All devices were tested under bias in a vacuum chamber for two to four weeks. During different portions of these tests, data were collected at temperatures near -25 C, +20 C and + 35 C. Many detectors were tested simultaneously. Leakage currents and noise were sampled at four minute intervals throughout.

4.1 SIS

Room-temperature leakage currents at the depletion bias ranged from below 1 μA, typical of the thinnest detectors, to ~4 μA for a fcw of the thicker devices. Usually, however, these did not scale with temperature in quite the way that would be expected for purely thermal generation within the bulk crystals Thus some surface leakage could be inferred. Nevertheless, currents were generally steady, rising very slightly or not at all during the scvcml-week-long tests.

Nearly every detector had an acceptable absolute noise level. Resolutions ranged between 50 and 200 keV FWHM, with the thicker (lower capacitance) devices generally having lower values. A few detectors displayed some noise instability with time in vacuum. These latter devices were disfavored when selections were made for the flight instrument,

Breakdown voltages measured after thermal-vacuum testing were generally within -10 V of those found before testing. Very fcw detectors were eliminated from flight viability as a result of drastically worsened characteristics. For roughly 1() % of the detectors, however, breakdown voltages improved by 30 V or more.

4.2 CRIS

In contrast to the oxide-passivatd S1S devices, our CRIS Si(Li) detectors displayed a variety of behaviors. Absolute currents started in the 10 – 25 μA range at room temperature, with single-groove detectors clustering more toward the lower values. Si(Li) currents generall y scaled even less distinctly with temperature than did those for I IPSi devices.

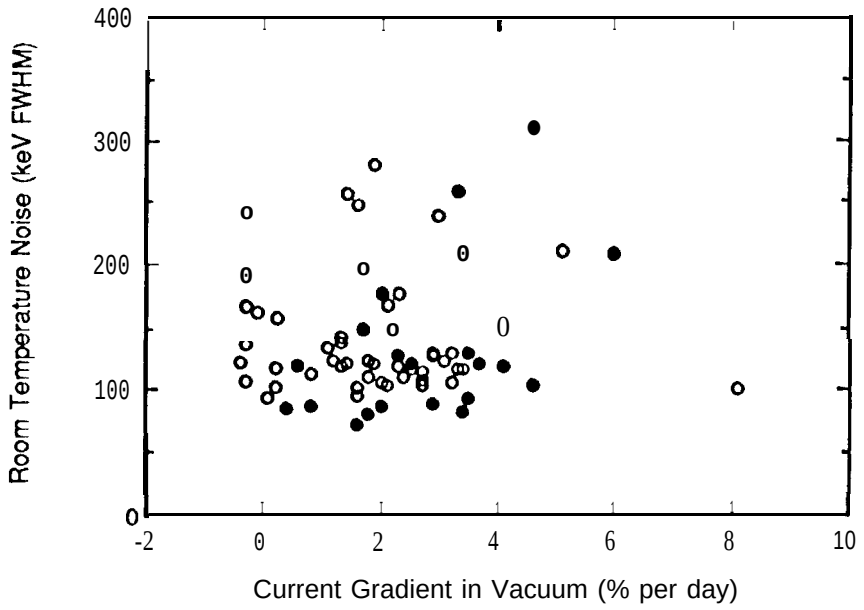

Figure 5. Noise versus leakage current growth for the CRIS Si(Li) detectors. Open and closed circles denote double and single groove detectors respectively. For flight, only those devices with gradients less than 4 % per day, and with noise levels below 220 keV were selected. Detectors with erratic, unstable noise characteristics have already been excluded from this plot.

Most significantly, leakage currents tended to grow with time in vacuum. Growth of -2 % per day was typical, but devices with gradients up to 8 % per day were found. (See Figure 5.) On the other hand, a few detectors showed current decreases of as much as 0.4 % per day. All such variations seemed largely unaffected by temperature. Currents for single-groove detectors tended to rise faster than those for double-groove devices, and many fewer of the former exhibited leakage decreases. The duration of onc thermal-vacutrm test was extended to over six weeks. Typical leakage current growth rates dropped from ~2 % per day to less than 1 % per day. Such gradients lead to acceptable absolute current levels; the CRIS instrument is expected to remain operable beyond the nominal two year mission objective.

Noise characteristics also showed a variety of different behaviors. As shown in Figure 5, typical full widths at half maxima were around 120 keV, but values up to 300 keV were found. Some devices were relatively quiet and stable. Others exhibited intermittent noise spikes, or other forms of instability. Single and double groove detectors had similar noise performance. Each detector could be rough] y ranked according to such performance, and these characteristics were strongly emphasized in selecting detectors for the flight instrument.

S. TOTAL THICKNESS

S1S and CRIS were designed to achieve rms isotopic resolutions of 0.3 arnu or better for stopping nuclei up through the iron group. To keep detector thickness errors from affecting this precision, the total thickness of each device must be known to better than 0.3 %. This converts to ≈0.3 μm for the thinnest HPSi detectors, and -9 μm for the Si(Li) detectors. Since thickness variations across these devices arc comparable to or larger than the allowable errors, especially for our S1S detectors, it was necessary to map the thicknesses as a function of position on each detector.

5.1 SIS

An interesting opportunity presented itself for measuring the relative thicknesses of our HPSi detectors, made possible by Lhcir rnirror-like, polished and metallized surfaces. A dual laser interferometer was developed at the Jet Propulsion Laboratory using commercially available components. The beam from a single laser was split into two separate Michelson interferometers, each measuring the distances, L_1 and L_2 from separate reference mirrors to the same spot on opposite sides of a detector wafer. Each wafer was scanned in a plane perpendicular to the two laser beams, which were themselves coaxially aligned. The sum L_1 + L2 should vary only because of wafer thickness variations, Since the measurements arc made simultaneously, this sum is insensitive to small movements of a detector along the direction of the beams. The resulting thickness maps were reproducible to within several tenths of a micron. Only a fcw detectors (typically 100 μm thick) were bowed enough to interfere with the laser mapping. Further details can be found in reference 6.

Absolute thickness calibrations were made using a mono-energetic beam of ^{36}Ar nuclei at the National Superconducting Cyclotron Laboratory at Michigan State University. The ^{36}Ar was sent through several selected spots on each detector, and stopped in well-charactcriz~d, thick E' detectors placed immediately behind, This beam, collimated to a -2 mm diameter, was also sent through the "slivers" of silicon wafers left over after orientation flats were cut off our detectors. Care was taken to avoid channeling, and subsequent energy-loss uncertainties, by orienting the beam away from crystal axes and planes,

The analysis of these measurements is not yet complete. It remains for us to make absolute determinations of the silicon sliver thicknesses, and to compare the corresponding E' energies with those made on our detectors. At the same time, our relative, thickness results from the interferometer studies will be checked.

5.2 CRIS

The surfaces of the Si(Li) detectors do not allow similar interferometric measurements to be taken. Wc therefore made complete thicknesses maps of these devices using the ^{36}Ar beam. Absolute calibrations were based on measurements made at selected points around the detectors with a capacitive thickness meter, which was in turn calibrated using precision silicon gauge blocks. Accuracies of -1 μm were achieved. Results for onc detector arc shown in Figure 6.

Total thickness gradients were typically less than -0.6 μm/mm from point to point around the Si(Li) wafers. Detectors with unusually large thickness gradients were avoided when selecting devices for inclusion in the flight instrument,

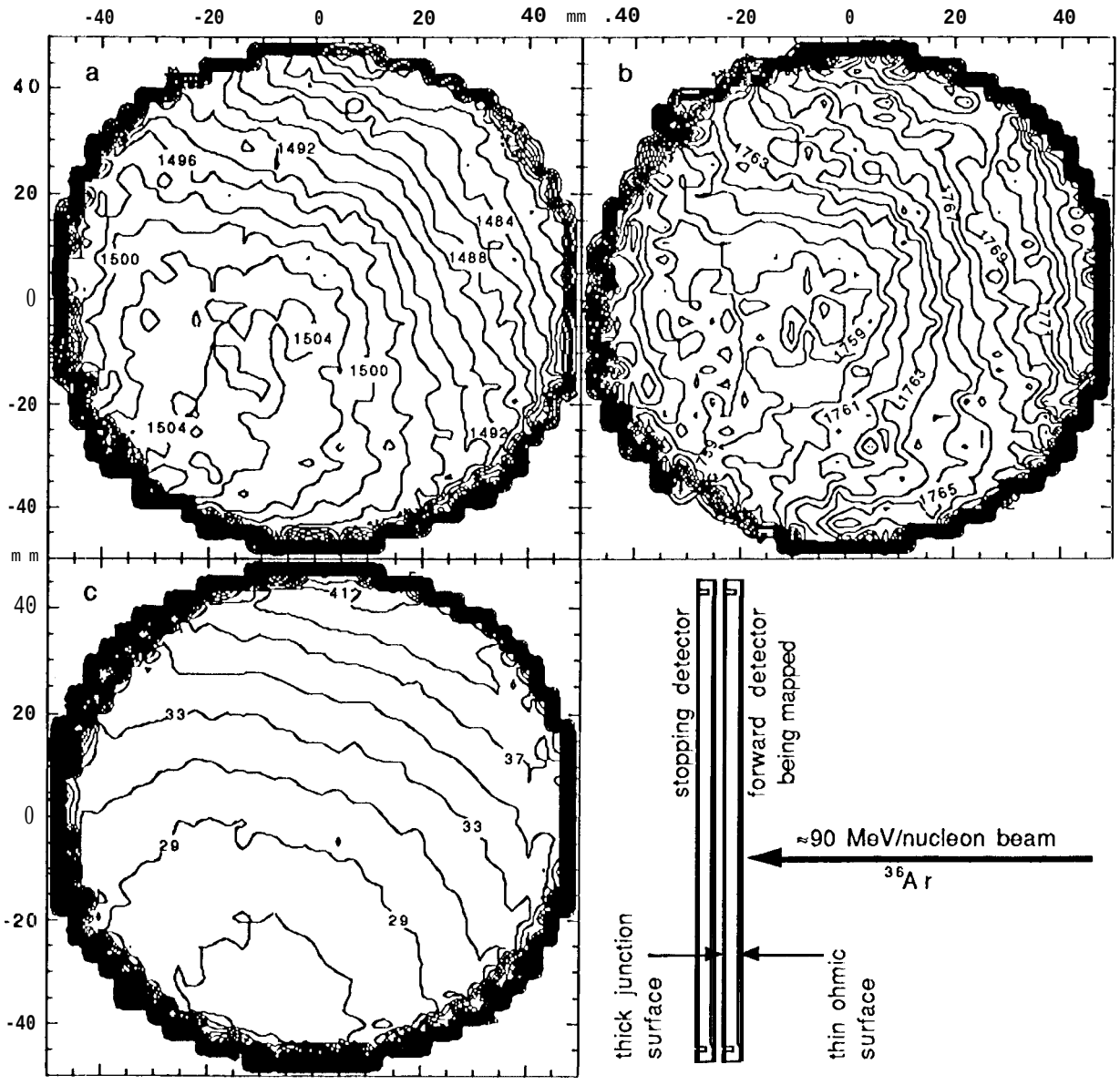

Figure 6. Measurements used to find the total and dead layer thicknesses for a particular CRIS detector. A low-intensity ^{36}Ar beam with energy around 3285 McV stopped in the second of two closely-spaced, coaxial Si(Li) devices. The entire front surface of this pair was sampled with over 100 particles pcr mm^2. Contours arc labeled with recorded energies in units of keV for the stopping (E') and forward (ΔE) detectors, in (a) and (b) respectively. The only dead layer encountered by the beam was on the exiting (junction) surface of the AE detector. The E' device was known to have a "flat" response when no absorbers were placed in front of it. Since the stopping power is ≈0.8 McV/μm for ≈1500 McV ^{36}Ar nuclei in silicon, lhc E' variations indicate total thickness differences for the ΔE detector of ≈2.4 pm pcr contour interval. Dead layer thicknesses were derived by comparing E'+ΔE with the total deposited energy expected in both detectors. These arc shown in (c), with contours labeled in units of microns of silicon. This particular device had dead layers that were somewhat thinner than usual,

6. DEAD LAYERS

Dead layers had to be measured to the same absolute resolution as were total thicknesses; i.e. ≈0.3 μm for the thinnest HPSi detectors, and -9pm for the Si(Li) detectors. Otherwise, the energy lost by a penetrating particle in a detector is not a wc,tl-determined fraction of that deposited in the active depth of that detector.

6.1 S1S

High-statistics ^{244}Cm maps of both the junction and ohmic surfaces were made with each HPSi detector biased near the voltage anticipated for flight: typically just -10 V below breakdown for the thicker devices, or at the corresponding voltage supply maximum for the thinner detectors. The alpha sources were collimated so that particles were incident at angles of less than 12° with respect to normal (mean ≈ 5.4°, rms ≈ 60), and dctczlor-source distances were adjusted to create alpha "spots" of ≈7 mm diameter. Over 1000 alpha events were accumulated at each of 103 locations on a triangular grid with 9 mm spacing. Thus, dead layers at each position were measured independently of those at nearby grid points.

Relative dead layer thickness maps were obtained by comparing the rccordcd pulse heights in these scans with the known stopping power of alpha particles in silicon. (For example, the contours in Figure 3 arc spaced by the silicon-equivalent of ≈0.2 μm dead-layer thicknesses.) The electronics gain was calibrated, and absolute dead layer measurements made, by comparing the pulse heights of alpha particles with two different energies from a similarly collimated ^{228}Th source incident on onc spot at the center of each detector surface. The encapsulations on each source were carefully investigated to eliminate errors duc to ill-determined alpha energies. As a consequence, typical rms uncertainties of better than 0.03 μm were achieved.

In general, dead layers were uniform on all detector surfaces, Those devices in which significant “features” remained were disfavored as possible elements in the flight stacks. Measured junction-side dead layers were in the range 0.31 ± 0.15 μm, while ohrric-side dead layers were in the range 0.24 ± 0.11 μm. There were indications that dead layers on the 100pm detectors were roughly 40 % thicker than those on other devices.

These results do not coincide with the nominal implantation depths noted above in section 2.1. In fact, the measured dead layers arc close to those anticipated duc to the aluminum metallizations alone. Such a finding was not expected, especially for the junction sides, where low-strength fields arc present. Onc possibility wc have considered is that the contacts arc partially “active”; i.e. some of the charge deposited in the junctions is collected in spite of the low field strength in these layers.

Alpha-particle measurements taken at lower bias, nearer depletion, indicated a general (~23 %) thickening of the apparent dead layers on both surfaces. This is equivalent to a -0.2 % decrement in charge collection efficiency. Losses may be occurring in the crystal bulk (due to trapping?) in regions where there arc low-strength electric fields. This hypothcsis will be checked against tests made using the ^{36}Ar beams, in which ΔE signals were recorded at different biases.

Finally, as another check on robustness, the fluence of ^{36}Ar was increased by a factor of -30000 at the center of onc 500 μm thick HPSi detector. Immediately after the exposure, which was accomplished in steps of increasingly higher fluxes, thc leakage current had risen by a factor of ~4. Subsequently, at room temperature, leakage currents were comparable from those taken before exposure, and no radiation-damage effects were visible in the alpha-particle maps of dead layers.

6.2 CRIS

Dead layer maps of our Si(Li) detectors were measured using -90 McV/nucleon beams of ^{36}Ar. (See Figure 6.) To avoid channeling, each detector was rotated 5° off axis (in both inclination and azimuth), with another, similarly rotated and well-studied CRIS stopping detector mounted just behind. The beam diameter was -1 cm, but the incident positions of individual particles were measured to within -1 mm by multi-wire proportional chambers located in front of our Si(Li) detectors. A square grid with 5 mm spacing was sampled, and over 100 particles pcr mm2 were accumulated everywhere on the detector surfaces.

Both the penetrated (ΔE) and stopping (E') detectors were oriented so that ^{36}Ar nuclei were incident on their ohmic surfaces. As noted above in section 2.2, ohmic contacts were made by depositing a thin layer of gold on the raw (etched) silicon surface. Consequently, the dead thickness of these contacts is very small. The only dead layer encountered by an

incoming ^{36}Ar nucleus therefore consisted of the heavily lithiated junction of the ΔE detector. This occurred a little over half way along the particle track: i.e. the ^{36}Ar stopped mid-way through the E' detector.

Dead layer thicknesses were measured by comparing the recorded energy sum, ΔE + E', with the total energy actually deposited, The latter was calculated from the total ^{36}Ar range: i.e. the known, total depth of the ΔE detector (L), together with the residual range in the E' detector (R'). Wc note that both L and R' arc derivable from E' alone; 1. is determined by the methods outlined in section 5.2, and R' is computed using range-energy curves found in the literature.[7]

Our rncasurcmcnts indicate generally uniform or slowly varying dead layers of average thickness 60 ± 17 μm. Local gradients as big as 0.69 ± 0.25 μm/mm (90^{th} percentile) were found. Very fcw detectors had small-scale regions with significant dead-layer deviations.

The measured dead layer thicknesses arc in agreement with that expected. Onc may compute the junction depth, given the fabrication steps of section 2.2: namely the drive-in diffusion time, compensation depth, and surface resistance after lapping. A heavily lithiated thickness of 55 – 70 pm is anticipated.

Our ^{36}Ar beam results arc in conflict, however, with dead layer thicknesses determined by other means, particularly low-energy alpha particles. To complete our study of the Si(Li) junctions, wc made measurements using the radioactive ^{228}Th source, which has prominent alpha particle lines at energies of 8784, 6778 and 6288 keV. Even though the ^{36}Ar beam measurements implied dead layers that were larger than the ranges of all alpha particles in the ^{228}Th decay series, spectra were obtained that included peaks from alphas of all energies. Wc suspect that charge collection efficiency varies within the. lithiated junction, Relatively more charge is collected for energy deposited nearer to the junction edge, c1osc to the start of the depletion region. Almost no charge is collected for energy deposits just next to the aluminized crystal surface. For energy deposits from heavy ions, in contrast to those from alpha particles, recombination 1osscs may be more significant and render nearly the entire junction dead. Further studies arc warranted.

7. CONCLUSIONS

A variet y of techniques were employed to thoroughly characterize HPSi and Si(Li) detectors intended for usc in the S1S and CRIS instruments aboard the ACE spacecraft. A fcw of the. most significant results arc summarized below.

Given the characteristics of available HPSi devices, and the selection criteria noted at the end of section 3.1, choices were made which resulted in the S1S layout shown in Figure la, High standards for full depletion were applied, and our options were severel y restricted by the range of viable voltages bet ween depletion and breakdown. This was especiall y true of devices over 500pm thick. Thus, while Iargc-area high-purity detectors can bc fabricated using standard techniques, yields arc limited by the availability of high quality silicon and the controls that must accompany manufacture.

A different appraisal must be made of the CRIS detectors. Device selections were limited by leakage and noise instabilities, and particularly by leakage growth in vacuum. Ncw fabrication techniques arc being sought to passivate the surfaces better.

Dead layers were found to bc non-trivial in character for both implanted HPSi and Si(Li) detectors. Depth-dcpcndcnt charge collection efficiency variations arc suspected, especially in the thicker lithiated junctions on Si(Li) detectors.

8. ACKNOWLEDGMENTS

This research was supported by the National Aeronautics and Space Administration at the California Institute of Technology (under contract NAS5-32626 and grant NAGW- 19 19), the Jet Propulsion Laboratory, and the Goddard Space Flight Center. BLD is grateful for support from the National Research Council. The Si(Li) detectors were fabricated at the Lawrence Berkeley National Laboratory, and the high-purity detectors were purchased from Micron Semiconductor, Ltd. of Sussex in the United Kingdom. Special thanks go to J. Walton, Y, Wong, C. Wilburn and A. Lucas for making these detectors. Wc thank G, Allbritton, M. Madden and B. Nahory for contributions in testing detectors and in taking data at MSU, as well as the personnel at the NSCL for their support. Wc also thank B. Scars for aid in analyzing this data.

9. REFERENCES

1. E. C. Stone, L. F. Burlage, A. C. Cummings, W. C. Feldman, W. E. Frain, J. Geiss, G. Gloeckler, R. E. Gold, D. Hovestadt, S. M. Krimigis, G. M. Mason, D. McComas, R. A, Mewaldt, J. A. Simpson, T. T. von Rosenvinge and M. E. Wiedenbeck, "The Advanced Composition Explorer", *The NASA Cosmic Ray Program of the 1990's and Beyond,* eds. W. V. Jones, F. J. Kerr and J. F. Ormes, pp. 48-57, Am. Inst. Phys. (Conf. Proc #203), Ncw York, 1990,

2. M. E. Wiedenbeck, E. R. Christian, W. R. Cook, A. C. Cummings, B. L. Dougherty, R. A. Leske, R. A. Mewaldt and T. T. von Rosenvinge, "Two-dimensional position-sensitive silicon detectors for the ACE Solar Isotope Spectrometer", *Gamma-Ray and Cosmic-Ray Detectors, Techniques, and Missions,* Vol. 2806, SPIE, 1996.

3. W. R. Cook, A. Cummings, B. Kccman, R. A. Mewaldt, D. Aalami, S. A. Kleinfelder and J. H. Marshall, "Custom Analog VLSI for the Advanced Composition Explorer (ACE)", *Workshop on Small Instruments for Space Physics, 1993.*

4. G. L. Allbritton, H. Andcrscn, A. Barnes, E. R. Christian, A. C. Cummings, B. L. Dougherty, L. Jensen, J. Lee, R. A. Leske, M. P. Madden, R. Mewaldt, B. Milliken, B. W. Nahory, R. O'Donnell, P. Schmidt, B. R. Scars, T. T. von Rosenvinge, J. T. Walton, M. E. Wiedenbeck and Y. K. Wong, "Large diameter lithium compensated silicon detectors for the NASA Advanced Composition Explorer (ACE) mission", IEEE Trans. Nucl. Sci., Vol. 43, pp. 1505-1509, June 1996.

5. Onc expects bulk current to scale as $e^{-E_{gap}/2kT}$. See A. S, Grove, *Physics and Technology of Semiconductor Devices, (Wiley, Ncw* York, 1967)

6. B. Milliken, R. A. Lcskc and M. E. Wiedenbeck, "Silicon Detector Studies with an Interferometric Thickness Mapper", 24th International Cosmic Ray Conference, Vol. 4, pp. 1283-1286, Rome, Sept. 1995.

7. J. F. Janni, "Proton Range-Energy Tables, 1 keV - 10 GeV", Atomic Data and Nuclear Data Tables, Vol. 27, pp. 147 – 529, 1982. See also F. Hubert, R. Bimbot and H. Gauvin, "Range and Stopping-Power Tables for 2.5-500 McV/Nucleon Heavy Ions in Solids", Atomic Data and Nuclear Data Tables, Vol. 46, pp. 1-213, 1990.